

A Simple Generalized Excitability Model Mimicking Salient Features of Neuron Dynamics¹

A. Giaquinta,² M. Argentina,² and M. G. Velarde²

Received December 9, 1999; final June 1, 2000

A generalization of the FitzHugh—Nagumo model for excitability is provided to account for salient features of Inferior Olive neurons. The base state is a limit cycle and excitability appears as spiking over peaks of the oscillations. The response of the model to various types of external stimulus is also presented. In particular, we show the relevance of an appropriate balance between amplitude and duration of the stimulus.

KEY WORDS: Excitability; subthreshold oscillations; spiking; Inferior Olive; neuron dynamics.

1. INTRODUCTION

Inferior Olive (IO) cells and other neurons exhibit autonomous, spontaneous and fairly robust regular quasi-harmonic oscillations that are called sub-threshold oscillations, with practically uniform amplitude and frequency throughout the IO.^(1–3) The behavior of these cells submitted to an external current, and various drugs has also been investigated and various threshold phenomena have been identified. Spontaneously or following a stimulus, onset, splitting and recreation of phase clusters of IO neurons have also been observed.

The effect of an external current can result in a violent response of the cell (and eventual emission of action potentials) before coming back to its sub-threshold oscillation or to rest. From a dynamical point of view, this phenomenon may be understood as a form of excitability. Generally, excitability has been considered when there exists a steady state and beyond a threshold, a strong enough perturbation yields a huge response

¹ Dedicated to Prof. G. Nicolis on his sixtieth birthday.

² Instituto Pluridisciplinar, Paseo Juan XXIII, no. 1, 28040 Madrid, Spain.

of the system after which it comes back to the original steady state.⁽⁴⁻⁶⁾ Here we consider the same phenomenon when the base state is oscillatory. We shall not deal with a strict comparison with experiment, but rather we shall concentrate on the qualitative properties of a model that we feel may prove useful in various other contexts besides IO neurobiology. Accordingly, the model that we are introducing now is in the spirit of recent publications devoted to a general discussion about the transition from oscillatory to spiking behavior in neurons.⁽⁷⁻⁹⁾

2. DYNAMICAL MODEL

The paradigmatic system exhibiting excitability is the well known FitzHugh–Nagumo (FHN) model,^(5, 6) a simplified albeit significant version of the Hodgkin–Huxley set of equations dealing with pulse propagation along axons.^(10, 11) The FHN equations are:

$$\begin{cases} u_t = (-v + f(u))/\varepsilon \\ v_t = -v + \alpha u \end{cases} \quad (1)$$

where $f(u) = -u(u-1)(u-\gamma)$ and the variables u and v mimic, respectively, the cross membrane potential and a recovery variable that captures the result of most of the significant ionic currents involved in the dynamics. The smallness parameter ε is the ratio between the two time scales associated with the corresponding time evolution of u and v . Loosely speaking, it is related to the high cell membrane capacity. For α sufficiently large, Eqs. (1) have a single fixed point, the origin, and it is linearly stable. A positive value of γ accounts for the threshold to destabilise the base state, for finite disturbances, thus leading to a significant large excursion in the (u, v) plane. The smallness of ε constrains the dynamics to a “pseudo invariant manifold,” i.e., $\mathcal{M} : v = f(u)$. In fact even small differences between v and $f(u)$ produce a rapid adjustment of u because of the small denominator in the evolution equation of this variable. The second equation promotes the slow change of v that tunes again u , as graphically illustrated in Fig. 1.

The above mentioned two-dimensional system can be modified in order to show oscillation and excitability, simply by changing the order of the polynomial function $f(u)$, in such a way that it possesses an extra minimum and an extra maximum (for this it is enough a fifth order polynomial).

Provided that the intersection of $f(u)$ and $v = \alpha u$ occurs between the first minimum and the first maximum, the model performs relaxation oscillations as in the van der Pol oscillator.⁽¹²⁾ Adding other minimum-

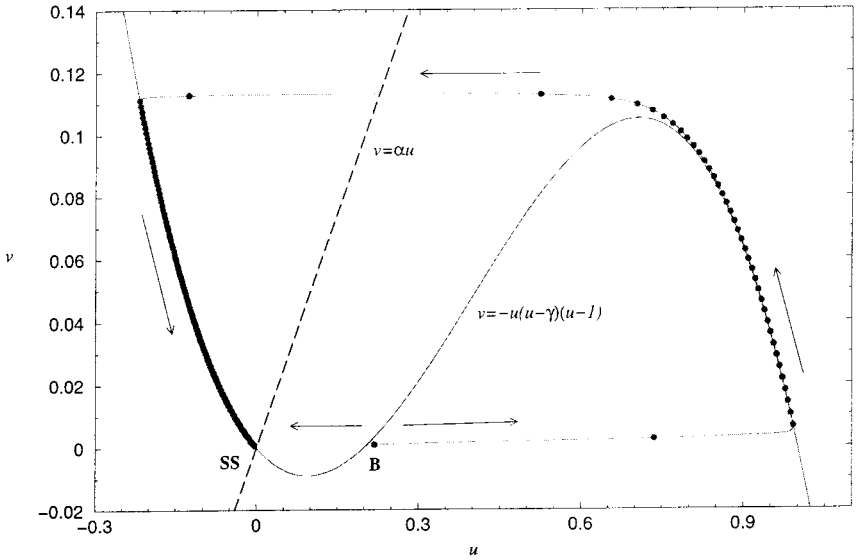


Fig. 1. Phase portrait (u, v) of a FHN system (Eqs. (1)) with parameter values $\varepsilon = 0.001$, $\gamma = 0.2$ and $\alpha = 0.5$. The points marked with the labels **SS** and **B** are respectively the steady state and the beginning of the trajectory. The continuous and dashed lines represent the graphs of the nullclines $\dot{u} = 0$ and $\dot{v} = 0$ respectively. The trajectory of the system is marked by a line with bullets at equal time intervals to highlight the differences in the velocity in different parts of the trajectory. Arrows show the direction of the flow.

maximum pairs, one could be also able to account for more than one instability threshold.

For reasons that will be clear further below, we choose a different approach. We add a third variable, w , to system (1). Our idea is to construct as a base state, a stable limit cycle, around the origin, lying on the three dimensional surface generated by \mathcal{M} . Accordingly, we consider the set of equations:

$$\begin{cases} u_t = (f(u) - v)/\varepsilon \\ v_t = Ar - \Omega w - r(r^2 + w^2) \\ w_t = Aw + \Omega r - w(r^2 + w^2) \end{cases} \quad (2)$$

with $r = v/\alpha - u$. This is one possible choice that satisfies our purpose.

Now, besides the origin $(0, 0, 0)$, if $\alpha < (1 - \gamma)^2/4$, we also have as steady states of Eqs. (2) $(u_{\pm}, \alpha u_{\pm}, 0)$, with $u_{\pm} = (1 + \gamma \pm \sqrt{(1 - \gamma)^2 - 4\alpha})/2$. For simplicity, however, we take Eqs. (2) with a single fixed point (the origin) and hence, α is taken high enough. The linear stability analysis

shows that the origin is stable when the parameter A is negative and large, in absolute value. For this range of parameter values, rescaling the time by $|A|$, so using $T = |A| t$, the system (2) reduces to a straightforward generalization of the FHN Eqs. (1):

$$\begin{cases} u_T = (f(u) - v)/(\varepsilon |A|) \\ v_T = u - v/\alpha \\ w_T = -w \end{cases}$$

Let us now come back to the system (2). The fixed point becomes unstable through an Andronov–Hopf bifurcation (AHB) when the following relation is verified:

$$-\gamma A \alpha (\gamma + \alpha + \gamma \alpha) + (A^2 (2\gamma \alpha + \gamma + \alpha + \alpha^2 \gamma) - \Omega^2 \alpha^2) \varepsilon + O(\varepsilon^2) = 0$$

Then, an oscillatory instability occurs when γ becomes negative as also expected for Eqs. (1). However, if we take γ greater than zero, there is an AHB at

$$A = -\frac{\Omega^2 \alpha}{\gamma(\gamma + \gamma \alpha + \alpha)} \varepsilon + O(\varepsilon^2)$$

The rationale behind the onset of this limit cycle is as follows. Due to the smallness of ε , the variable u in the neighborhood of the origin becomes slaved by v . As a consequence, the first equation of system (2) decouples from the second and the third ones. In this limit, the latter two equations become:

$$\begin{cases} r_t = \beta[(A - (r^2 + w^2))r - \Omega w] \\ w_t = (A - (r^2 + w^2))w + \Omega r \end{cases} \quad (3)$$

with $\beta = 1/\alpha + 1/\gamma$. Note that Eqs. (3) appear like the normal form of an AHB. This system (3) undergoes the AHB when $A = 0$, and the frequency of the expected limit cycle at onset is $\nu = \Omega \sqrt{\beta} + O(\varepsilon)$. The phase portrait near the AHB is sketched in Fig. 2a. The mentioned limit cycle represents the sub-threshold oscillation of the IO cells.

As ε is small, the oscillatory flow is confined to the transversal neighborhood (of size ε) of the manifold \mathcal{M} . Near this transition, the oscillation is quasi-harmonic, and the amplitude of the oscillation increases like \sqrt{A} . When the limit cycle approaches the local minimum of \mathcal{M} , a drastic change in the time evolution is expected. An estimate of the threshold of this transition is obtained by finding when the amplitude of the limit cycle

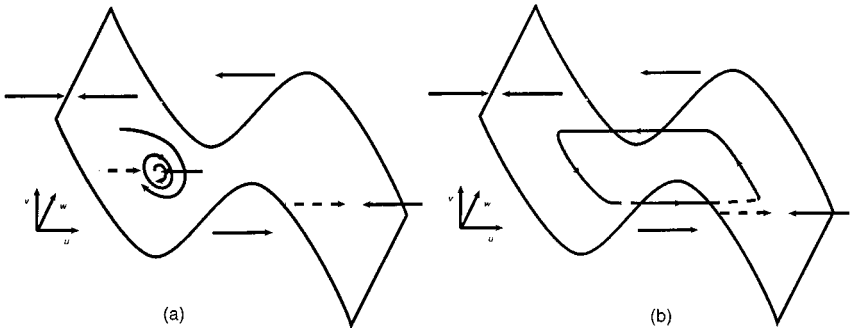


Fig. 2. Sketch of the phase portrait (u, v, w) of the system (2) when the controlling parameter Ω is small enough. (a) Parameter values near onset of the limit cycle (subthreshold oscillations). (b) Relaxation oscillation regime (excitable oscillations).

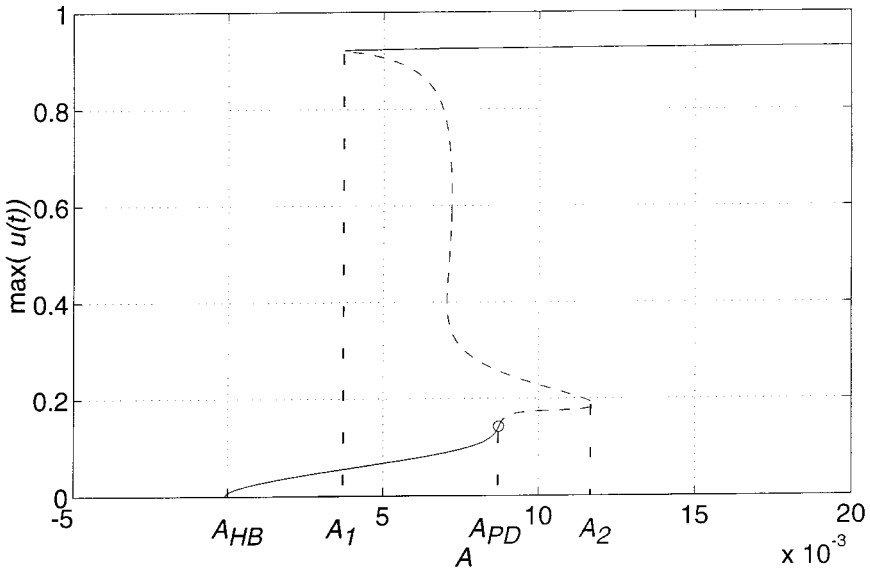


Fig. 3. Bifurcation diagram of periodic solutions for the system (2). The maximum of the first variable, u , is plotted as function of the value of the parameter A . The unstable (resp. stable) branches are drawn with dashed (resp. solid) lines. The instability occurring at the point marked with a circle, A_{PD} , corresponds to a period-doubling bifurcation. The lower (resp. upper) stable branch corresponds to sub-threshold (resp. spiking) oscillations. Parameter values: $\epsilon = 0.02$, $\gamma = 0.2$, $\Omega = 0.04$, and $\alpha = 0.3$.

becomes equal to the curvilinear arc distance on the cubic surface separating the origin from the local minimum, u_1 , of \mathcal{M} .

Since we predict the disappearance of the sub-threshold oscillations, we expect the presence of another attractor. A potential attractor corresponds to the relaxation oscillation between the branches of the manifold \mathcal{M} , giving rise to the spiking oscillations that are characteristic for the system (1) (Fig. 2b). Increasing the value of A helps the onset of the spiking oscillations.

The qualitative picture presented above has been quantitatively checked by numerically integrating Eqs. (2). Using the software *auto97*,⁽¹⁴⁾ we performed a continuation of the quasi-harmonic periodic orbit, when the value of the controlling parameter A is changed. A typical bifurcation diagram is shown in Fig. 3.

The sub-threshold oscillation becomes unstable when the parameter A becomes large enough, typically through a period doubling. With parameter values as in Fig. 3 the period doubling occurs at $A = A_{PD} \simeq 8.7 \cdot 10^{-3}$. Between $A = A_1 \simeq 3.7 \cdot 10^{-3}$ and $A = A_2 \simeq 1.2 \cdot 10^{-2}$, the system shows bistability between the (limit cycle) subthreshold oscillations and the spiking.

As the aim of this work is to find a regime of parameter values where the subthreshold oscillations are excitable, we take A in the range $A_{HB} < A < A_1$ for which we refer to our generalization of excitability. Note that, depending on the values of the other parameters, the subthreshold oscillations may not yield to excitability, as A_1 can be lower than A_{HB} .

When the controlling parameter, A , becomes slightly higher than A_{PD} , Eqs. (2) may exhibit irregular behavior (Fig. 4). One of the Lyapunov exponents is slightly positive: $(6.5 \pm 0.5) \cdot 10^{-3}$ for the values of parameters corresponding to Fig. 4. This attractor is therefore chaotic.

Let us emphasize the role of the third variable added to Eqs. (1). First of all, while in the model presented above we have a single parameter governing the AHB and its continuation, namely A , in a two-variable model such as

$$\begin{cases} u_t = \left(-v + \sum_{i=1}^5 a_i u^i \right) / \varepsilon \\ v_t = -v + \alpha u \end{cases} \quad (4)$$

the bifurcation parameter would be a_1 but, proceeding in the supercritical region, the coefficients a_i ($i = 2, \dots, 5$) become drastically relevant and hence we cannot continue the bifurcation diagram following only the first coefficient, a_1 , as in Fig. 3. On the other hand, in system (2) the parameter Ω is selecting the frequency of subthreshold oscillations, while in system (4)

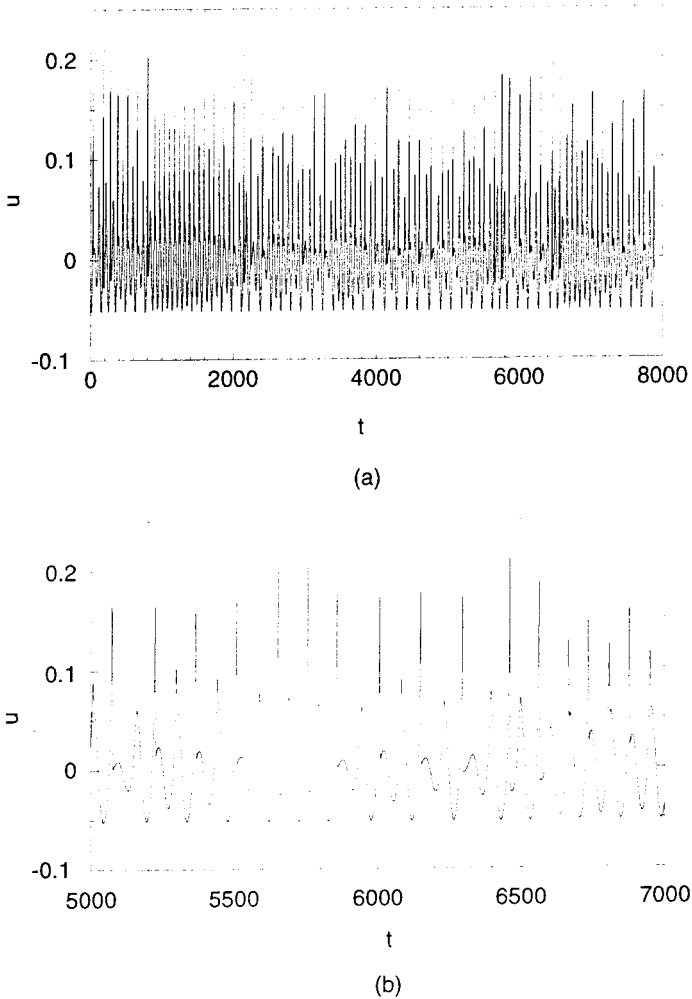


Fig. 4. (a) Irregular time series (b) is an enlargement of (a). Parameter values: $\varepsilon = 4 \cdot 10^{-2}$, $\gamma = 0.2$, $\Omega = 0.035$, $\alpha = 0.5$, and $A = 7.058 \cdot 10^{-3}$.

there is no way to change the frequency of spiking and the one of sub-threshold oscillations separately.

3. RESPONSE OF THE DYNAMICAL SYSTEM TO AN EXTERNAL STIMULUS

Let us investigate the behavior of model (2) when an external stimulus is provided. As u is loosely related to the cross-membrane potential, it

seems natural to model an external input $\mathcal{J}(t)$ by an extra term in the first equation of (2)

$$\begin{cases} u_t = (f(u) - v)/\varepsilon + \mathcal{J}(t) \\ v_t = Ar - \Omega w - r(r^2 + w^2) \\ w_t = Aw + \Omega r - w(r^2 + w^2) \end{cases} \quad (5)$$

We will refer to $\mathcal{J}(t)$ as either “the stimulus” or “the current” without really going beyond the mere analogy of model (5) with an underlying physiological system. When $\mathcal{J}(t)$ is constant, if the sign of the current is positive (resp. negative), the cell is said to be depolarized (resp. hyperpolarized). The main effect of this stimulus is a shift of the manifold \mathcal{M} , by an amount equal to $\varepsilon\mathcal{J}(t)$. As a consequence, the intersection of the nullclines (the fixed point) is also displaced. Various forms of the stimulus, namely constant, Heaviside step function and square signals have been considered.

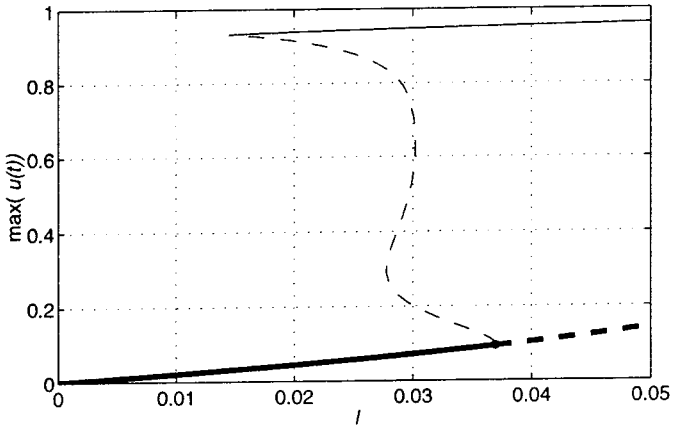
3.1. Continuous Stimulus

The numerical continuation of the base state—that may be either the fixed point or the limit cycle—shows that there exists a critical value of the continuous stimulus, \mathcal{J}^* , that leads to the instability of the rest state, as shown in Fig. 5. Assume that $A_{HB} < A < A_1$, so that the base state is a limit cycle. From now on, we restrict consideration to a parameter regime near the AHB. When the intensity of the external stimulus is increased, the location of the limit cycle on \mathcal{M} changes. For $\mathcal{J} = \mathcal{J}^*$, the limit cycle reaches the local minimum u_1 , and thus becomes unstable.

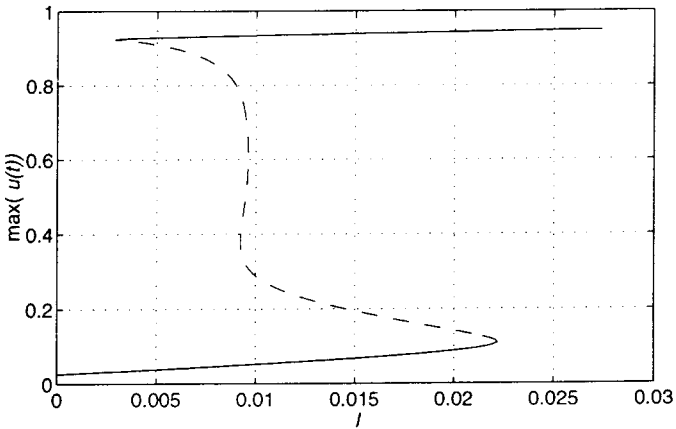
3.2. Heaviside Stimulus

A constant current is applied at $t = 0$. If the stimulus amplitude is small, the system just relaxes to the sub-threshold oscillations, i.e., to the limit cycle, but there also exists a critical amplitude of the injected current, namely \mathcal{J}_1 , which forces the system to produce a spike before returning to the quasi-harmonic oscillation. The excitation is favored when u is near its maximum (or v minimum). This is a consequence of how the model (5) was built. We can give an estimate of the value of \mathcal{J}_1 simply taking into account that the smallness of ε produces a trajectory almost parallel to the u -axis, so, in the most favourable case, i.e., v is in its minimum, we would have to provide a quantity at least

$$\mathcal{J}_1 \simeq (\min\{v(t)\} - f(u_1))/\varepsilon$$



(a)



(b)

Fig. 5. Bifurcation diagram obtained when a continuous stimulus is applied to the system. In both panels, for computational convenience, we have scaled quantities with the numerical value given to ε , hence the abscissa runs as $I = \varepsilon \mathcal{J}$ with $\varepsilon = 0.02$. (a) $A = -10^{-2}$, the only attractor is a fixed point when $\mathcal{J} = 0$. The thick line corresponds to the branch of the fixed point. The thin line is the branch of limit cycles. (b) $A = 10^{-3}$, the only attractor is a limit cycle when $\mathcal{J} = 0$. The critical current corresponds to the forcing value that leads to instability of the rest state.

Actually this is not sufficient because, although the flow was initially below \mathcal{M} (i.e., $v < f(u)$), the system may cross again the central branch of the manifold \mathcal{M} —that is like an ignition barrier—, before coming back to its rest state. When the flow approaches the barrier, the system is more excitable. Such a feature has been experimentally observed with IO cells *in vitro*.⁽¹⁻³⁾ The minimal distance from the flow location to this barrier can be considered as an excitability measure.

3.3. Square Stimulus

A constant current is applied for $0 < t < T$. When the stimulus is applied, depending on its amplitude \mathcal{J} and its duration T , the model (5) shows responses that are typical of excitable systems. A stimulus of too short duration, even with a high current intensity, may not excite the system. Furthermore, whatever the length of the time duration of the stimulus, if its amplitude is below \mathcal{J}_1 , no excitation can occur. Thus, the significant quantity is the appropriate balance between the amplitude and the duration of the stimulus. When the value of ε tends to zero, the response is instantaneous, as the characteristic time evolution of u scales with ε . The system is excited if at the end of the stimulus, the flow has reached a point on the other side of the barrier. We have checked these heuristic results by numerically integrating the Eqs. (5). In numerical experiments, guided by what has been measured in experiments,⁽²⁾ we have also considered a parameter regime such that the period of subthreshold oscillations is about three times the period of the spikes. We choose $\varepsilon = 0.02$, $\gamma = 0.2$, $\Omega = 0.04$, and $\alpha = 0.3$. For a square signal stimulus, two thresholds appear, one correlates with the duration of the stimulus and the other with the amplitude. For example, when the amplitude of the stimulus is 0.5, for a time duration $T = 0.53$, no excitation of the system is observed, whereas for $T = 0.54$, we observe a spike as a response to the stimulus. When the duration of the stimulus is 2.0, there exists a critical value, $\mathcal{J}_1(T)$, that excites the system ($\mathcal{J}_1(T) \simeq 0.32$ in Fig. 6).

Note that the response of the model depends also on the time instant when the stimulus is applied. As already said, at the peak of the oscillations of u , it is easier to excite the system (Fig. 6b). Note the “rebound” after the spiking shown in Fig. 6b which is characteristic of the IO cells.⁽²⁾ This rebound spike is associated in our model to the return to the oscillatory base state.

3.4. Metastable Spiking After a Stimulus

In experiments⁽²⁾ a single stimulus can produce a train of two or more spikes even if the stimulus lasts less than the spike duration. This can be

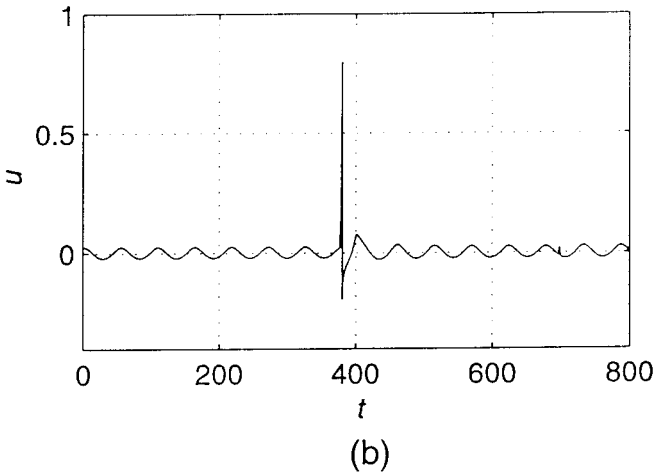
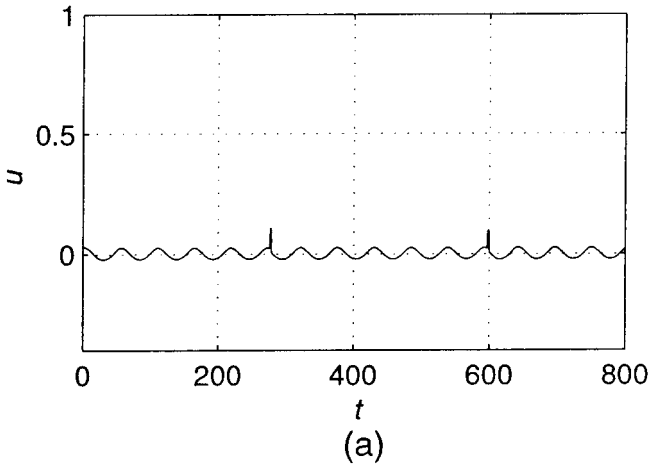


Fig. 6. Response of Eqs. (5) to an external stimulus at two instants of time. (a) When $t = 277$ and $t = 597$, a stimulus of amplitude 0.32 and duration 2 is applied. No significant response is observed. (b) When $t = 377$ and $t = 697$, a stimulus of amplitude 0.321 and duration 2 is applied. We observe a response to the first stimulus, but not to the second. The difference between the two excitations is that the first one is applied at the peak of the signal u , and the second off-peak.

interpreted as a kind of “metastability” of the spiking solution. We can observe this behavior also in system (5) choosing parameter A close to (and smaller than) A_1 . In this regime of parameter values the spiking solution is not yet a stable limit cycle, as it appears at $A = A_1$ via a saddle-node bifurcation of limit cycles. Nevertheless, the flow may be trapped during a

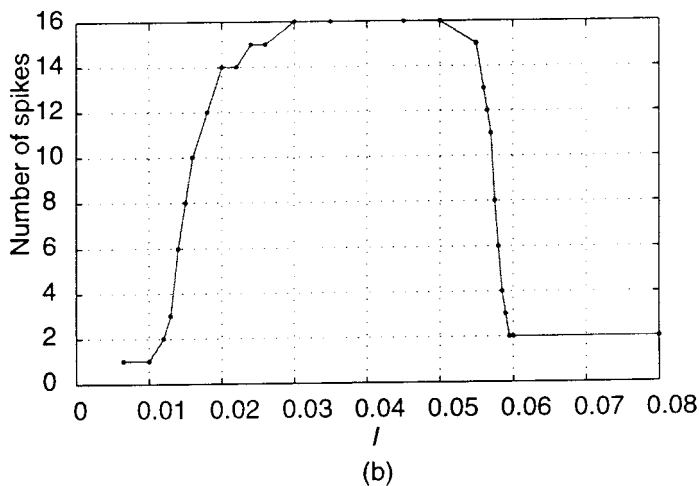
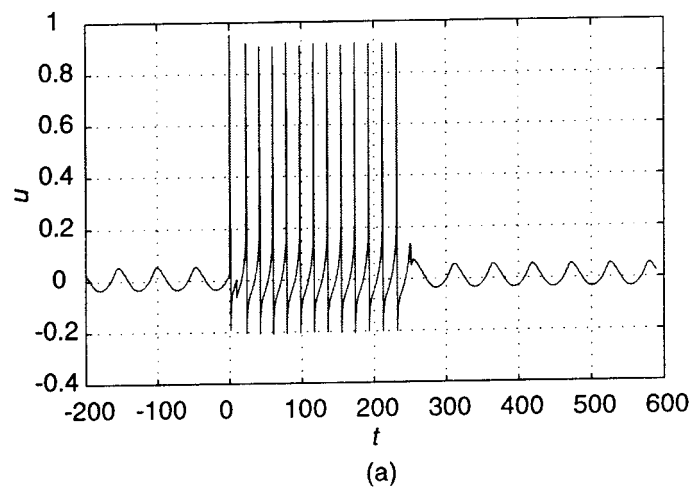


Fig. 7. Response of Eqs. (5) to a square stimulus for the parameter regime near the appearance of the spiking oscillations. The stimulus is applied at $t=0$, and has a duration $T=10$. As in Fig. 5, for mere computational purpose, we scale \mathcal{J} with the actual numerical value given to ε , hence we use $I = \varepsilon \mathcal{J}$. (a) Metastable spiking obtained for $I=0.018$. (b) Number of spikes as a function of the amplitude of the stimulus. Parameter values: $\varepsilon = 0.02$, $\gamma = 0.2$, $\Omega = 0.04$, $\alpha = 0.3$.

finite time in the region of the appearance of the new attractor as if the system were reminiscent of its existence. This can also happen for A close to (but higher than) A_1 . However, in this case, as there is bistability, a stimulus of appropriate time duration and intensity can also put the system in the still small basin of attraction of the spiking solution.

A multiple-spike response to a stimulus is presented in Fig. 7a. The dependence of the number of spikes, as a function of the stimulus intensity, is shown in Fig. 7b. There exists a finite range of values of \mathcal{J} leading to metastable spiking. For values of \mathcal{J} less than $\mathcal{J}_1(T)$ no spike is observed. Increasing \mathcal{J} the number of spikes produced by a single stimulus grows up to a "saturation" value. Further increase of the current intensity produces a bifurcation at $\mathcal{J} = \mathcal{J}_2$ such that the line $v = \alpha u$, $w = 0$ intersects the manifold $v = f(u) + \varepsilon \mathcal{J}$ in the central (unstable) part and hence the number of spikes depends only on the duration of the stimulus. Eventually, for \mathcal{J} very large, the intersection occurs in the second stable branch of the manifold and hence a stable limit cycle appears. The stimulus produces an overshooting followed by a relaxation to the limit cycle.

4. CONCLUSION

We have provided a natural generalization of the excitability concept long ago introduced by FitzHugh and others and we have shown it helps understanding, at least to a qualitative albeit significant level, some salient features of the IO neuron dynamics. The model exhibits spiking behavior upon an oscillatory (limit cycle) base state.

We feel that, in view of the geometrical approach here taken, the model we have studied may prove useful in other realms of neurobiology, nonlinear science and engineering.

ACKNOWLEDGMENTS

The authors acknowledge enlightening discussions with Profs. R. R. Llinás, L. Fortuna and P. Arena. This work has been supported by the Spanish Ministry of Education and Culture (Grant PB 96-599) and by the EU (TMR Grant FMRX-CT96-0010). Part of the numerical simulations have been performed thanks to the NLKit software developed at Institut Non-Linéaire de Nice.

REFERENCES

1. R. Llinás and Y. Yarom, *J. Physiol.* **315**:569 (1981).
2. R. Llinás and Y. Yarom, *J. Physiol.* **376**:163 (1986).

3. L. S. Benardo and R. E. Foster, *Brain Res. Bull.* **17**:773 (1986).
4. For a survey see E. Meron, *Pattern Formation in Excitable Media* (Springer, New York, 1992).
5. R. FitzHugh, *Biophys. J.* **1**:445 (1961).
6. J. S. Nagumo, S. Arimoto, and S. Yoshizawa, *Proc. I.R.E.* **50**:2061 (1962).
7. X. Wang and J. Rinzel, in *The Handbook of Brain Theory and Neural Networks*, M. Arbib, ed. (MIT Press, 1995), pp. 686–691.
8. H. D. I. Abarbanel, M. I. Rabinovich, A. Selverston, M. V. Bazhenov, R. Huerta, M. M. Sushchik, and L. L. Rubchinsky, *Physics-Uspeski* **39**:337 (1996).
9. H. Haken, *Principles of Brain Functioning* (Springer-Verlag, Berlin, 1996).
10. A. L. Hodgkin and A. F. Huxley, *J. Physiol.* **177**:500 (1952).
11. J. Cronin, *Mathematical Aspects of Hodgkin–Huxley Neural Theory* (Cambridge University Press, Cambridge, 1987).
12. B. van der Pol, *London, Edinburgh and Dublin Phil. Mag.* **3**:65–80 (1927).
13. H. A. Braun, H. Wissing, K. Schäfer, and M. C. Hirsh, *Nature* **367**:270 (1994).
14. E. J. Doedel, H. B. Keller, and J. P. Kernévez, *Int. J. Bifurcation Chaos* **1**:3, 493 (1991).